

Review Article

Properties and Microstructures of Sn-Bi-X Lead-Free Solders

Fan Yang,¹ Liang Zhang,^{1,2} Zhi-quan Liu,² Su-juan Zhong,³ Jia Ma,³ and Li Bao³

¹School of Mechanical and Electrical Engineering, Jiangsu Normal University, Xuzhou 221116, China

²Institute of Metal Research, Chinese Academy of Sciences, Shenyang 110016, China

³State Key Laboratory of Advanced Brazing Filler Metals & Technology, Zhengzhou Research Institute of Mechanical Engineering, Zhengzhou 450001, China

Correspondence should be addressed to Liang Zhang; zhangliang@jsnu.edu.cn

Received 29 June 2016; Revised 18 October 2016; Accepted 23 October 2016

Academic Editor: Peter Majewski

Copyright © 2016 Fan Yang et al. This is an open access article distributed under the Creative Commons Attribution License, which permits unrestricted use, distribution, and reproduction in any medium, provided the original work is properly cited.

The Sn-Bi base lead-free solders are proposed as one of the most popular alloys due to the low melting temperature (eutectic point: 139°C) and low cost. However, they are not widely used because of the lower wettability, fatigue resistance, and elongation compared to traditional Sn-Pb solders. So the alloying is considered as an effective way to improve the properties of Sn-Bi solders with the addition of elements (Al, Cu, Zn, Ga, Ag, In, Sb, and rare earth) and nanoparticles. In this paper, the development of Sn-Bi lead-free solders bearing elements and nanoparticles was reviewed. The variation of wettability, melting characteristic, electromigration, mechanical properties, microstructures, intermetallic compounds reaction, and creep behaviors was analyzed systematically, which can provide a reference for investigation of Sn-Bi base solders.

1. Introduction

As is known to all, Sn-Pb solders which are thought of as traditional solders have been widely applied in the field of electronic packaging for many decades. Concerning the toxicity of Pb to human health and environment [1–3], many countries have limited or banned the production and application of Sn-Pb solders in many fields by means of legislations. For example, WEEE and RoHS were conducted in Europe [4, 5]. Thus the substantial attention of both scientists and engineers who wish to find a type of unique solder which could replace Sn-Pb solders has been attracted to the lead-free solders.

In recent twenty years, lead-free solders have made great development and several main kinds of Sn-based lead-free solders such as Sn-Ag [6, 7], Sn-Zn [8, 9], Sn-Bi [10, 11], Sn-Cu [12, 13], and Sn-Ag-Cu [14, 15] have been fiercely studied by researchers. Among these most promising lead-free solder alloys, however, the Sn-Bi solder alloys have better properties such as lower melting temperature, good tensile strength, good reliability, and well creep resistance [16–18]. The eutectic Sn-58Bi solder has a low melting point of 139°C [19, 20] and it is lower than 183°C of the eutectic Sn-Pb solder which consists of 63 wt.% Sn and 37 wt.% Pb [21, 22]. At the same time,

the cost of Sn-Bi solder is lower than others [23]. However, two main problems limiting the application of the Sn-Bi base solders in the electronic packaging are the frangibility and poor ductility [24].

In this paper, the effects of adding alloy elements including Al, Cu, Zn, Ga, Ag, In, Ni, Sb, nanoparticles, and rare earth to the Sn-Bi solders on the properties and microstructures of Sn-Bi solders were systematically discussed and some suggestions were put forward to handle these problems in improving the properties of the Sn-Bi solders.

2. Wettability

Wettability is one of the extremely critical characteristics playing a key role in evaluating the soldering technology of lead-free solders [25]. It is defined as an ability which is the spreading property of molten solder spreading over on the substrate during the reflow process [26]. At the same time, wettability also is considered the capacity of molten solder to react with a substrate to form a IMC layer which is the bonding between the solder and the substrate [27]. The wettability of Sn-58Bi solder performs worse than that of the Sn-Pb solder which includes Pb element [28], whereas adding alloy elements to the Sn-Bi solders is an effective

means of improving the wettability. Generally, there are two frequently used methods including the wetting balance method and spreading method which are used for evaluating the wettability.

Li et al. [29] have done research on the effect of a small amount of Al addition on the wettability of the Sn-58Bi solder. Due to Al being too active or the flux being not matched to this solder, it was found that the wettability of the Sn-58Bi solder became poorer after adding 2 wt.% Al to the eutectic Sn-58Bi solder. Miao et al. [30] indicated that the addition of 1.0 wt.% Cu did not influence critically the wettability of the Sn-58Bi solder. Compared with the of the Sn-58Bi solder, the contact angle of the Sn-Bi-1Cu solder alloy on various metal foils and metallized substrates changed slightly. Zang et al. [31] carried out wetting test for Sn-30Bi-0.5Cu solder at different temperatures. At 220°C, the contact angles which were used to determine the extent of wetting changed critically from 150° to 30°, but the wettability of Sn-30Bi-0.5Cu changed slightly at 275°C and 350°C, especially at 350°C. At 275°C and 350°C, the contact angles maintained about 28° and 20°, respectively. The spreading ratio (S_R) was calculated as follows [32]:

$$S_R = \frac{D - H}{H} \times 100\%, \quad (1)$$

where H stands for the height of solders after spreading and D stands for the diameter of solder balls. Zhang et al. [32] using resin flux and organic flux in the spreading test found that with the Sb content changing the spreading ratio changed along two irregular curves at 190°C and all reached the summit when Sb content was at 2.0 wt.%. The highest spreading ratio was 78.2% and it was higher than that of Sn-58Bi solder. Chen et al. [33] studied the wettability of Sn- x Bi-3Zn ($x = 37, 38, 39, 41, 42, 43$) and Sn-38Bi- x Zn ($x = 0, 23, 4$) at 170°C and 190°C. At 170°C, the spreading ratio was increased from 68% to 72% with the Bi element increased; but the spreading ratio was decreased from 75.8% to 66% and then increased to 72.7% with the Zn element increased. At 190°C, the spreading ratio of the Sn- x Bi-3Zn alloys was decreased from 73.2% to 72% and then increased to 73.3% and it was higher than that at 170°C. However, the spreading ratio of the Sn-38Bi- x Zn alloys changed slightly remaining 72% at 190°C. The wettability of the Sn-58Bi, Sn-35Bi-0.5Ag, and Sn-35Bi-1.0Ag was investigated by Zhang et al. [34]. The above three solders with different fluxes showed different wettability with air and N₂ atmosphere. The Sn-35Bi-1.0Ag solder showed the best wettability because its wetting angle was the smallest with air and N₂ atmosphere.

By adding nanosized Y₂O₃ to the Sn-58Bi solder, it could be found that the spread area of the composite solder alloy was increased by 20% from 30 mm² to 36 mm² and then declined to 32 mm² with the addition of Y₂O₃ nanoparticles added from 0 to 3.0 wt.% [35]. The wettability of the Sn-58Bi solder with 1.0 wt.% Y₂O₃ nanoparticles was best. Liu et al. [36] reported that the wettability of the Sn-58Bi composite solder with the addition of Cu₆Sn₅ particles (0.5 wt.% and 1 wt.%) was worse than that of the Sn-58Bi solder. Liu also made a conclusion that the spread area of the Sn-58Bi with 1 wt.% Cu₆Sn₅ particles was reduced by 10% compared to that

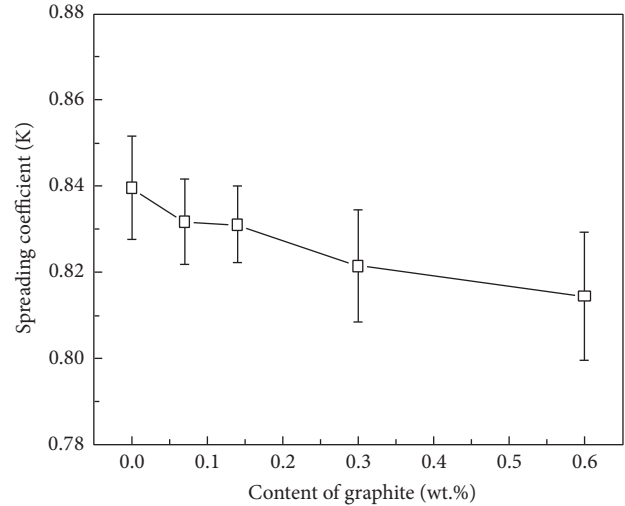


FIGURE 1: Effect of nanosized graphite on the spreadability of Sn-Bi composite solder [37].

of Sn-58Bi solders after reflowing for 30 min. Similarly, as can be seen from Figure 1 [37], the wettability of the composite solders was weakened with the increasing addition of nanosized graphite. The spreading coefficient was decreased from 84% to 81%.

Dong et al. [25] proposed the effect of the addition of Ag and RE (primarily Ce and La) on the wettability of the Sn-58Bi solder. It could be seen that adding 0.5 wt.% Ag or 0.1 wt.% RE improved the wettability of the Sn-58Bi solder, but the effect of adding a little amount of RE elements is superior. The spreading area of Sn-58Bi0.1RE was increased by 15% from 66 mm² to 76 mm² and it was more 3 mm than the spreading area of Sn-58Bi0.5Ag. When Dong et al. added simultaneously 0.5 wt.% Ag and 0.1 wt.% RE to the Sn-58Bi solder, compared to the spreading area of the Sn-58Bi-0.5Ag solder, the spreading area of the Sn-58Bi0.5Ag0.1RE composite solder increased about by 14% from 73 mm² to 83 mm².

3. Melting Characteristic

In the microelectronic package, the solder joint is a critical part. Similarly, the melting temperature is a critical characteristic for low-temperature solders [24]. In recent years, low melting point alloys which are suitable for applications in soldering with lead-free materials have attracted an increasing technological interest [38]. To use a low melting point solder is an important approach to strengthening solder joint reliability [39], because low melting temperature soldering is potential that electrical devices to be soldered are prone to thermal damage [40]. For example, flexible board, LED, LCD, and air conditioning safety protector need lower soldering whose temperature is lower than 183°C of the eutectic temperature of Sn-Pb solder. The melting point of the eutectic Sn-58Bi solder alloy is 139°C [41]. To develop the lead-free solder database, the thermodynamic data is very significant [42].

Compared with the prominent endothermic peak for the pure Sn-58Bi solder, the prominent endothermic peak for the

TABLE 1: Melting temperature of Sn-58Bi-based solder alloys ($^{\circ}\text{C}$) [25].

Solder	Sn-58Bi	Sn-58Bi-0.5Ag	Sn-58Bi-0.1Ag	Sn-58Bi-0.5Ag-0.1RE
Solidus	136.1	135.7	136.2	136.6
Liquidus	139.1	138.2	139.7	139.1
Mushy zone	3	2.5	3.5	2.5

Sn-58Bi solder with addition of 3 wt.% Al was increased up to 142°C [43]. Shen et al. [44] adding 0.1 wt.% Cu and 2 wt.% Zn to the Sn-Bi solder found that the melting temperature of the Sn-40Bi-0.1Cu composite solder was 132.2°C . It was lower than the melting temperature of the Sn-58Bi solder, but the melting point of the Sn-40Bi-2Zn-0.1Cu solder was increased slightly up to 136.3°C . Addition of Cu could reduce the melting temperature, but Zn addition has the opposite effect. Ma and Wu [45] also found that the solidus and liquidus temperatures of the Sn-58Bi solder with the addition of 0.7 wt.% Zn elements was decreased compared that of the Sn-58Bi solder and the melting point of the Sn-58Bi-0.7Zn solder was 136.3°C . At the same time, Chen et al. [33] considered that the melting temperature of the Sn- x Bi-2Zn ($x = 38, 40,$ and 44) alloys was 136.7°C , 136.5°C , and 137.3°C , respectively, and it was lower than that of the Sn-58Bi solder. When the content of Zn element occupied 3 wt.%, the melting temperature of the Sn- x Bi-3Zn ($x = 39, 41$ and 43) alloys was 138.0°C , 137.0°C , and 136.8°C , respectively. It also has been reported that adding 3 wt.% Zn could decrease the melting point of the Sn-Bi solder because the melting temperature of the Sn-32at.% Bi-3at.% Zn solder was 130.8°C [46]. The melting temperature of the Sn-Bi solder with 0.04 wt.% Cu addition was changed slightly because the melting point of the Sn-58Bi-0.04Cu solder was 138.65°C . Lin et al. [47] offered a concrete analysis of the effect of adding the Ga element (from 0.25 wt.% to 3.0 wt.%) to the Sn-58Bi solder on liquid point of the Sn-58Bi solder. The results indicated that the addition of Ga element changed slightly the liquid points which was around 150°C . Adding 0.5 wt.% Ag and 0.1 wt.% RE also had little effect on melting temperature of the Sn-58Bi solder as shown in Table 1 [25]. It could be seen that the solidus temperature and the liquidus temperature of the Sn-58Bi-0.5Ag were lowest compared to that of other solders. So it implied that the addition of Ag element could reduce the melting temperature of the Sn-58Bi solder, but the RE operated an opposite behavior.

Shalaby [48] found that the addition of In elements had critical effect on the onset point of the Sn-58Bi solder which meant that adding 2 wt.% In could decrease the onset point of the solder from 139.06°C to 129.68°C . But the onset point of the Sn-58Bi solder with addition of 2 wt.% Ag elements did not change remaining at 139.06°C . So it was considered that the 2 wt.% Ag addition had little effect on the onset point of the Sn-58Bi solder. At the same time, adding 2 wt.% In and 2 wt.% Ag to the Sn-58Bi solder reduced the melting temperature of the composite solder from 143.75°C to 133.59°C . Zhang et al. [34] pointed out that the effects of the 0.3 wt.% and 1.0 wt.% Ag addition on the solid phase line temperature of the Sn35Bi solder were slight because the

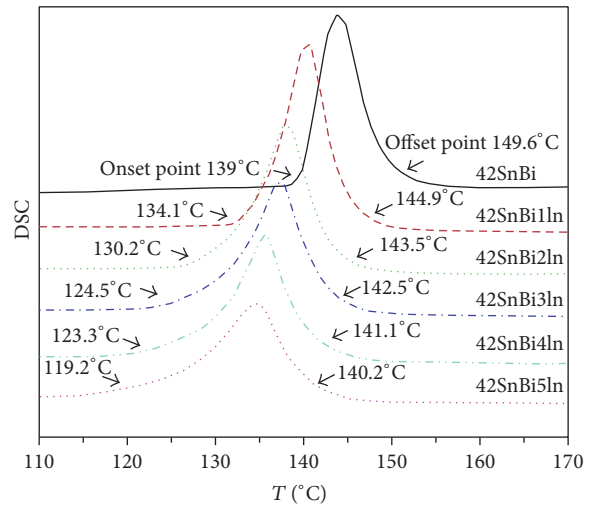


FIGURE 2: DSC curve of Sn-Bi-In alloys [24].

solid phase line temperatures of the Sn35Bi, Sn35Bi0.3Ag, and Sn35Bi1.0Ag composite solders were 138.5°C , 138.8°C , and 138.9°C , respectively. But the liquidus temperature of the above solders was 150.3°C , 183.6°C , and 184°C ; it could be seen that the effects of the 0.3 wt.% and 1.0 wt.% Ag addition on the liquidus temperature were obvious. Chen et al. [24] studied the effects of In addition on the melting temperature of Sn-Bi solder. Figure 2 showed that adding 1 wt.% In caused about 5°C decline of the onset point and 1°C decrease of the offset point. When the content of In addition was 5 wt.%, the onset point was decreased about 20°C . With increasing In content, the peak temperature of the composite solder was reduced by 10°C . Zhang et al. [32] added Sb element to Sn-48Bi solder and found that all the main peaks appearing around 147°C . The discovery also revealed that the melting range and liquidus temperature reached the maximum when the addition of Sb was at 1.8 wt.% and then began to drop with the Sb content increased. In addition, when the addition of Sb element did not change which is at 1.8 wt.%, the melting range and melting temperature increased with Bi content decreased.

Huang and Chen [49] indicated that the addition of the 0.05 wt.% and 0.5 wt.% Co elements showed slight effects on the onset point and peak point of the Sn-57Bi solder because the onset points and peak points of the three types of solders were 140.3°C , 140.3°C , and 140.1°C and 143.5°C , 144.2°C , and 142.5°C , respectively. Liu et al. [35] studied the effect of different additions of Y_2O_3 nanoparticles on the melting temperature of the Sn-58Bi solder. It was found that the melting temperature of the pure eutectic Sn-58Bi solder was 138.77°C , but it did not change greatly ranging from

138.83°C to 139.2°C after adding 0.5, 1.0, and 3.0 wt.% Y_2O_3 to the Sn-58Bi solder, respectively. In the meantime, adding SiC nanoparticles which were 45–55 nm also did not influence the melting temperature of the Sn-58Bi solder largely [50]. Peng and Deng [51] also found that the melting point of the Sn-Bi with reduced grapheme oxide nanosheets (RGOS) was 139°C.

By DSC analysis, it was evidenced that the addition of 0.5 wt.% La element could reduce the melting temperature of the Sn-58Bi solder because the Sn-58Bi and Sn-58Bi-0.5La solders had eutectic points of 138.60°C and 137.84°C, respectively [52]. Wu et al. [53] revealed that adding RE (primarily Ce and La) ranging from 0.25 wt.% to 1.0 wt.% to Sn-57Bi-1Ag solder did not critically change the solidus and liquidus temperatures which were still about 136°C and 139°C, respectively, but the mushy temperature zone was increased slightly from 2.7°C to 3.9°C.

4. Electromigration

Electromigration is defined as atomic diffusion driven by high electric current flow [54]. In electronic industry, high current density which may cause some failures in solder joints was demanded [55, 56]. In addition, electromigration affects the phase formation at the joint interface, the phase coarsening, and mass accumulation of Bi in the solder. So electromigration (EM) which has been widely regarded as the most critical reliability problem causing hillock formation has become an issue which was discussed aggressively in electronic packaging [57]. He also revealed that Bi layers were formed at the anode interface indicating that Bi was the main diffusing species migrating from the cathode to the anode. When Sn-Bi base solder joint is under current stressing, Bi atoms migrate along the direction of electron flow and accumulate at the anode side [58]. However, it has been found that the diffusion processes of the Bi atoms may be changed by adding alloying elements which could cause less Bi segregation [59].

L.-T. Chen and C.-M. Chen [60] investigated that microstructure evolution and interfacial reaction in the eutectic SnBi solder joint on the Ni/Au metallization with and without the current stressing of 6.5×10^3 A/cm² at 70°C for 5 to 15 days. Without the current stressing, only a thin Ni_3Sn_4 phase was found at the joint interface. When the solder joint was added current stressing, a thick Au-Ni-Bi-Sn phase was formed after 10 days. However, the new phase disappeared at the anode-side joint interface after 15 days of current stressing. Chen and Huang [61] did research on the effect of the addition of 0.5 wt.% Ag on the electromigration of the Sn-58Bi solder and found that the formation of Ag_3Sn could intercept the Bi migration from the cathode side to the anode side. Doping the reactive nanoparticles into the plain Sn-58Bi solder is a good choice to improve the mechanical performances of the Sn-58Bi solder ball [62]. Xu et al. also investigated the effect of addition of microsized Ni particles on the electromigration of the Sn-58Bi solder. It was revealed that the Ni particles functioned as barriers to stall the Bi atoms which were considered as the dominant diffusion entities leading to a decline of the mean velocity of Bi atoms during the current stressing.

5. Mechanical Properties

As we all know, Sn-Bi base solders show brittle behavior which may be fatal to electronic products. But the tensile and shear strength of Sn-Bi base solders are superior to those of the Sn-Pb solders and Sn-Bi base solder joints show better reliability [63]. Compared with the mechanical properties of lead-free solder joints, the Sn-Bi base solders are not best. Now, to improve mechanical properties of Sn-Bi base solders we can add impurity elements to the solders by refining solders' microstructure [64].

5.1. Tensile Property. Shen et al. [44] reported that the mean tensile strength of the Sn-58Bi solder was 73.24 Mpa. But after adding 0.1 wt.% Cu to the Sn-40Bi solder the mean tensile strength was increased by 12.6% up to 82.45 MPa. The mean tensile strength of the Sn-40Bi solder with 2 wt.% Zn and 0.1 wt.% Cu was increased by 21.9% up to 89.31 MPa. At the same time, compared with the Sn-58Bi solder, the Vickers hardness of the Sn-40Bi-0.1Cu and Sn-40Bi-2Zn-0.1Cu solders was increased by 15.0% and 19.9%, respectively, which could be said that adding Cu and Zn elements strengthened the Vickers hardness of the Sn-Bi solder. Ma and Wu [45] added Zn element to the Sn-58Bi solder. The ultimate tensile strength of the Sn-58Bi solder with Zn elements addition ranging from 0 to 2.0 wt.% was increased from 59 MPa to 63 MPa and then decreased to 52 MPa during reflow soldering. Similarly, during liquid-state aging, the UTS of Sn-58Bi-*x*Zn solder slabs was increased from 62.6 MPa to 66 MPa and then decreased to 55.7 MPa. It was seen that the UTS was highest when the Zn content was at 0.7 wt.% during reflow soldering and liquid-state aging. Sakuyama et al. [65] studied the effect of adding a third element including Ag, Cu, Zn, and Sb on tensile strength of the Sn-Bi solder. At high strain rate (3 mm/min), adding 0.5 wt.% Ag element to the Sn-58Bi solder increased the tensile strength by 13.2% up to 86 MPa and the elongation was improved by 80%. The additions of 0.5 wt.% Cu and Sb elements changed the tensile strength slightly. However, the effect of Cu and Sb addition on elongation was pronounced. The elongation was enhanced by 140% and 320%, respectively. The addition of 0.5 wt.% Zn weakened the tensile strength of the Sn-58Bi solder decreased to 68 MPa and changed the elongation slightly.

Kubota et al. [66] also added 0.5 wt.% Sb element to the Sn-58Bi solder. The effect of the 0.5 wt.% Sb addition on the tensile strength of the Sn-58Bi solder was different at various temperature. At 25°C, the tensile strength of the Sn-57.5Bi-0.5Sb solder was increased from 67 MPa to 90 MPa, but that of the Sn-58Bi solder ranged from 72 MPa to 100 MPa as the time increased; At 80°C, the tensile strength of the Sn-57.5Bi-0.5Sb solder was increased all time up to the highest 50 MPa while the tensile strength of the Sn-58Bi solder was decreased to 38 MPa and then increased to 70 MPa higher than that of the Sn-57.5Bi-0.5Sb all time; At 120°C, the tensile strength of the Sn-58Bi and Sn-57.5Bi-0.5Sb solder was decreased compared with that at 25°C and 80°C. It indicated that the effect of 0.5Sb addition on the tensile strength of the Sn-58Bi solder was larger at higher temperature than that at lower temperature. Ma and Wu [67] added grapheme nanosheets

TABLE 2: Shear strength of Sn-Bi-Sb/Cu joints [32].

Alloy	Shear strength/MPa
Sn-58Bi	55.5
Sn-52Bi-1.8Sb	53.0
Sn-48Bi-1.4Sb	45.2
Sn-48Bi-1.8Sb	45.8
Sn-48Bi-2.0Sb	47.1
Sn-48Bi-2.4Sb	66.7

(GNSs) to Sn58Bi0.7Zn solder and found that the UTS of the Sn58Bi0.7Zn- x GNS ($x = 0, 0.038, 0.076$ and 0.114 wt.%) solder joints was decreased after aging at 150°C for various times (20, 40, 60, 80, 100, and 120 min). But it could be found that the UTS of Sn58Bi0.7Zn with 0.076 wt.% GNSs addition was almost the highest at the same aging time and it was decreased from 62.7 MPa to 51.7 MPa. However, the UTS of Sn-58Bi was the lowest all the time and it was decreased from 58.9 MPa to 50.6 MPa.

Similarly, Chen et al. [24] studied the effect of In addition on tensile properties of Sn-Bi-In solder alloys. The results implied that the tensile properties of the Sn-Bi solder with addition of In element were poor decreasing from 71.8 MPa to 68.3 MPa when the content of the In addition was at 3 wt.%. Then the tensile strength of the Sn-Bi-3In solder was increased to 69.2 MPa. In contrast, however, the effect of In addition on the elongation firstly was positive than worse. When the content of In addition was at 2.5 wt.%, the elongation was highest increased by 104.5%. Shalaby [48] not only added In element to the Sn-58Bi solder, but also added Ag element to the Sn-58Bi solder. Compared with the Sn-58Bi solder, the tensile and shear strength of Sn-58Bi-2In, Sn-58Bi-2Ag and Sn-58Bi-2In-2Ag were increased by 6.5%, 8.0%, 12.1% and 6.7%, 8.1%, 12.9%, respectively. When Sb element was added to the Sn-Bi solder, the shear strength of the composite solder was first decreased and then increased with the Sb addition increased as shown in Table 2 [32]. It was revealed that the shear strength of the Sn-48Bi-1.4Sb was lowest. When the content of Sb addition was at 2.4 wt.%, the shear strength was increased by 20.2% compared with that of the Sn-58Bi solder.

5.2. Shear Property. Dong et al. [25] studied not only the effect of Ag element, but also effect of RE (primarily Ce and La) element on the shear strength of the Sn-58Bi solder. It was obviously shown that adding a small quantity of Ag and RE elements could increase the shear strength of the Sn-58Bi-based solder joints as reflowed or after thermal aging. However, in the as-reflowed condition, the shear strength changed slightly. The shear strength of the Sn-58Bi, Sn-58Bi-0.1RE, Sn-58Bi-0.5Ag, and Sn-58Bi-0.5Ag-0.1RE almost remained at 81 MPa. Nevertheless, after aging for 168 h at 80°C , the shear strength of all the solder joints was 70 MPa, 80 MPa, 75 MPa, and 80 MPa, respectively. The addition of trace amounts of RE elements improved the shear strength of Sn-58Bi base solders and reduced the effect of high-temperature aging on shear strength highly. In fact, adding RE resulted in the increase in

the fraction of net-like eutectic and the decrease in the size of the IMCs. Mokhtari and Nishikawa [59] found that adding 0.5% or 1% In element could improve the shear strength, but the effect of Ni additions was negative. It was appreciable to be seen that the shear strength of the Sn-58Bi-1In and Sn-58Bi-0.5In was higher and the shear strength of the two solders remained at about 70 MPa after reflow or 6 weeks of aging time at 80°C . But the Sn-58Bi with 0.5 and 1 wt.% Ni additions showed lower shear strength after reflow or 6 weeks of aging time at 80°C due to the segregation of Bi resulting in the large Bi phases. The low shear strength of Sn-Bi base solders with Ni addition could be attributed to the segregation of Bi which led to the large Bi phases.

Shafiq et al. [43] found that adding Al nanoparticles to the Sn-58Bi solder led shear strength of the new Sn-58Bi-3Al composite solder higher than that of the Sn-58Bi solder consistently. When substrate was Cu, the shear strength of the Sn-58Bi and Sn-58Bi solder with 3.0 wt.% Al nanoparticles was decreased from 31.5 MPa to 24.5 MPa and from 33 MPa to 27 MPa, respectively, as aging time increased at 75°C ; But when substrate was Au, the shear strength of the two solders was decreased from 30 MPa to 22.2 MPa and from 30.5 MPa to 26.5 MPa, respectively. The Al doped Sn-58Bi solder had higher shear strength because of a second phase dispersion which strengthened mechanism and refined β -Sn microstructure. Additionally, due to the presence of the Cu_6Sn_5 IMC, the shear strength of solders with Al nanoparticles in Cu pad was higher than the Au pad. Liu et al. [36] performed shear tests on Sn-58Bi/Cu, SB-0.5 Cu_6Sn_5 /Cu, and SB-1 Cu_6Sn_5 /Cu samples and found that the effect of adding Cu_6Sn_5 particles to Sn-58Bi solder on mechanical properties was critical. And it was clearly seen that the shear strength of composite solder joints was strengthened to be higher than that of Sn-58Bi/Cu. The shear strength of the Sn-58Bi, SB-0.5 Cu_6Sn_5 , and SB-1 Cu_6Sn_5 was 44.7, 48, and 61.9 MPa, respectively, when shear rate was $9 \times 10^{-3} \text{ s}^{-1}$. It was increased by 7.4% and 38.5%, respectively. When shear rate was $9 \times 10^{-2} \text{ s}^{-1}$, the shear strength was 59.2, 64.7, and 66 MPa increased by 9.3% and 11.5%, respectively. The strengthening effect can be due to the dispersive distribution of Cu_6Sn_5 powers. Hu et al. [62] found that when Al_2O_3 nanoparticles were added to Sn-58Bi solder, the shear strength of the new composite solder and the plain solder was decreased from 93.2 MPa and 91.8 MPa to 85.0 MPa and 83.0 MPa after experiencing 288 h aging time at 85°C . In addition, the shear strength of the new solder was better than that of the plain solder at the same aging time. At the same time, the microhardness was also decreased from 24.5 HV and 24.2 HV to 20.1 HV and 18.6 HV, respectively, as the aging time added. What is more, Yang et al. [37] concluded that adding nano-sized graphite weakened the average ultimate tensile strength of the Sn-58Bi solder. The average ultimate tensile strength of the Sn-58Bi solder was 57.75 MPa and it was higher than that of the Sn-58Bi solder with nanosized graphite. When content of graphite was at 0.14 wt.%, the average ultimate tensile strength of the composite solder was lowest, namely, 52.5 MPa. However, the elongation of Sn-Bi with 0.07 wt.% nanosized graphite was highest up to 2.019 μm . He et al. [68]

found that the UTS of the Sn-58Bi composite solder with 0.03%, 0.06%, and 0.1% CNTs was higher than that of the Sn-58Bi solder, but the UTS was decreased with the addition of CNTs increased. The UTS of the Sn-58Bi-0.03CNTs was the highest which reached 94.24 MPa. The shear strength of the Sn-58Bi solder with the addition of Y_2O_3 ranging from 0.5 wt.% to 3.0 wt.% was increased compared with that of the Sn-58Bi solder. The shear strength of the Sn-58Bi solder was about 28 MPa, but that of the SB-0.5 Y_2O_3 was increased to 31 MPa. The shear strength of the Sn-58Bi solder with the addition of 1.0 wt.% Y_2O_3 was increased critically by 50% up to 42 MPa and similar to that of the SB-3.0 Y_2O_3 [35]. The SiC nanoparticles were also incorporated into the Sn-58Bi solder [50]. The shear strength of the Sn-58Bi solder with SiC nanoparticles additions was increased to 95, 85, and 74 MPa during 0, 100, and 400 h for aging, respectively. The growth rates were 9.2%, 7.5%, and 12.1%, respectively. It was considered that the shear strength was decreased as aging time increased. Peng and Deng [69] proposed that the shear modulus of Sn-Bi/Graphene composite lap shear joint was increased from 12 GPa to 23 GPa with the increasing weight fraction of grapheme by finite element simulation. Peng and Deng [51] indicated that the incorporation RGOS played a positive role in enhancing the shear strength because the Sn-Bi/RGOS nanocomposites showed higher shear strength than the pure Sn-Bi solder.

Rare earth elements have been seen as the vitamins of metals [54] and adding trace amount of rare earth (RE) to improve their properties is considered as an effective way [70], because rare earth elements have high chemical activity and special and chemical properties [71]. But by adding 0.5 wt.% La to the Sn-58Bi solder, the ball shear strength of the Sn-58Bi-0.5La solder was lower than that of the Sn-58Bi solder and the former was less about 2.4 N than the latter [52]. It also exhibits that the bonding strengths of both Sn-58Bi and Sn-58Bi-0.5La solder joints are very stable during aging time at 75 or 100°C.

5.3. Creep Property. Researchers have evaluated the creep behavior of Sn-Bi alloy by various techniques including tensile, lap shear, and indentation analysis [72]. Sn-58Bi solder's creep resistance is better than that of the eutectic Sn-Pb solder at a temperature range between 20 and 70 [40].

The dependence of steady-state creep rate $\dot{\epsilon}$ can be characterized using the Dorn power equation in the following form:

$$\dot{\epsilon} = A_1 D_0 \frac{Gb}{RT} \left(\frac{b}{d}\right)^p \left(\frac{\sigma}{G}\right)^n \exp\left(\frac{-Q}{RT}\right), \quad (2)$$

where $\dot{\epsilon}$ is the creep rate; D_0 is a constant; G is the shear module; b is the Burgers vector; d is the grain size; σ is the applied stress; n is the stress exponent; A_1 and p are constants energy; R is the gas constant; T is absolute temperature. The solders are frequently subjected to large cyclic strains during normal service. In addition, thermally activated creep is an important reliability issue because of the high homologous temperature ($T/T_m > 0.5$) of solders [54].

For Sn-58Bi samples, the Bi-rich phase coarsened forming an obstacle and dislocations disappeared under the

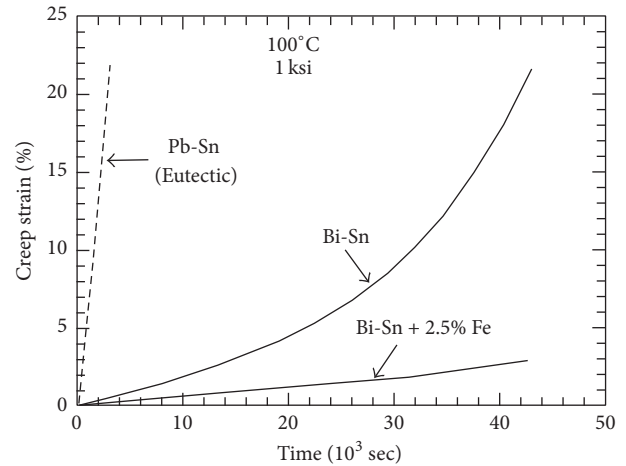


FIGURE 3: Comparative creep deformation at 100°C and 1 ksi [73].

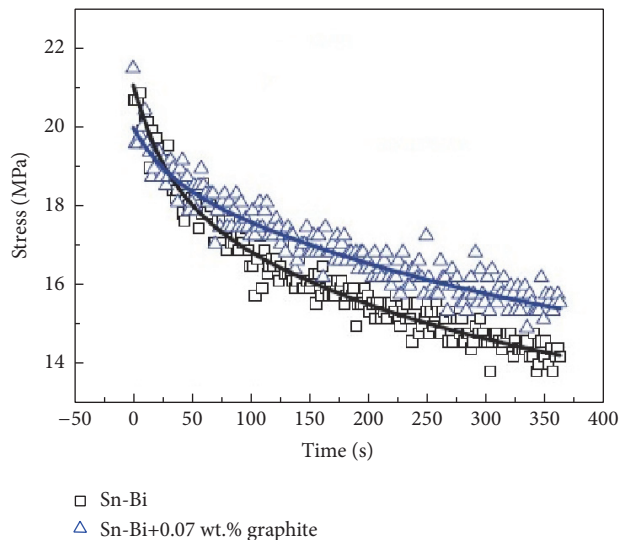


FIGURE 4: Stress relaxation curves of Sn-Bi and Sn-Bi+0.07 wt.% graphite composite solder [37].

stress bypassing these obstacles, leaving a dislocation loop surrounding each grain resulting in creep deformation, but the addition of Zn could suppress the coarsening of Bi-rich phase, leading to higher creep resistance [45]. The Sn-58Bi-2In-2Ag composite solder owned higher creep resistance than that of the Sn-58Bi solder [48]. Similarly, adding 2.5% Fe to Sn-57Bi solder exhibits that its creep resistance is superior than that of Sn-57Bi and Sn-Pb solder at 100°C and 1 ksi as shown in Figure 3 [73].

In Figure 4, compared to the stress relaxation rate of Sn-Bi+0.07 wt.% nanosized graphite solder joint, it was clear to see that the stress relaxation rate of Sn-58Bi solder joint was larger [37]. In other words, the creep rate of the Sn-Bi+0.07 wt.% nanosized graphite solder was lower than that of the Sn-58Bi solder. In Figure 5 [74], they selected 200 Mpa and 100 Mpa to represent the high stress and low stress regions. The pristine SnBi alloy showed the highest strain rate

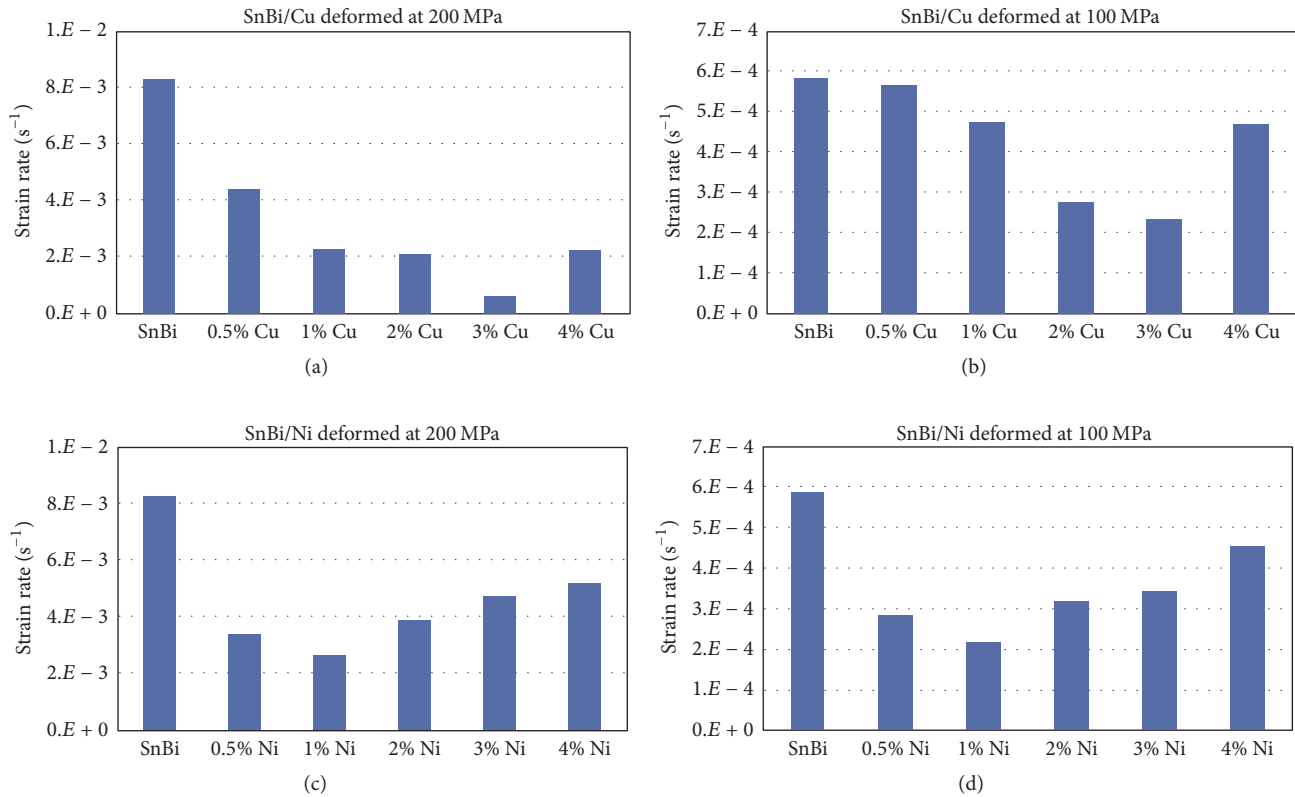


FIGURE 5: Strain rates of SnBi(Cu) alloys deformed at (a) 200 MPa and (b) 100 MPa. Strain rates of SnBi(Ni) alloys deformed at (c) 200 MPa and (d) 100 MPa [74].

(lowest creep resistance) at both stress levels. With addition of nano-Cu and Ni, however, the creep rate reduced critically and achieved best creep resistance when filler concentration reached 3 wt.% for Cu and 1 wt.% for Ni filler composite.

6. Microstructure of Solder Bulk

The Sn-58Bi solder exhibits an evident disadvantage which is the coarsening of the microstructure that could result in poor mechanical properties during thermal aging [75] and adding alloy elements could suppress the Bi segregation [59]. The thermodynamic modeling of the Sn-Bi system was carried out firstly by Ohtani and Ishida and Niu et al. [76] and the microstructure of the Sn-58Bi solder was typical lamellar eutectic structure made up of alternate-layered white Bi phase and grey Sn phase [24].

Miao and Duh [40] carried out experiments on effect of 1 wt.% Cu addition on the microstructure of the Sn-58Bi solder. The mean intercept length of the Bi-rich phases was increased from $1.01 \mu\text{m}$ to $4.80 \mu\text{m}$ by 375.2% during different aging times which were 0, 4, 9, 16, 25, and 36 days. However, the number only was increased to $1.09 \mu\text{m}$ after the 1 wt.% Cu element added to the Sn-58Bi solder. It indicated that the Cu addition could refine the microstructure of the Sn-58Bi solder. A study about the effect of 1.0 wt.% Cu addition on the microstructure of the Sn-58Bi solder was undertaken [77]. The microstructure of the Sn-58Bi solder was refined by adding 1 wt.% Cu after 3 days of aging at 80°C . Because

the addition of Cu element slowed down the microstructure coarsening of the Sn-58Bi solder. Mokhtari and Nishikawa [59] found that a large Bi phase was detected in Sn-Bi-1Ni solder alloy after reflow and Bi coarsening happened clearly after 6 weeks of aging. However, it did not find a clear sign of Bi segregation in the eutectic Sn-Bi and Sn-Bi-1In solder alloys. In addition, after 6 weeks of aging, adding 1 wt.% In element to the Sn-58Bi solder could refine the microstructure of the Sn-58Bi solder.

In Figure 6 [65], it was shown that only adding 0.5 wt.% Zn to the Sn-Bi solder increased the average grain size of microstructure of the Sn-58Bi solder about by 5.2%. However, adding other alloy elements could refine the microstructures. The average grain size of the Sn-58Bi solder was decreased by 30.4% after adding 0.5 wt.% Ag. Adding 0.5 wt.% Cu element decreased the average grain size by 26.1%. The addition of Sb affected critically the average grain size decreasing the average grain size to $1.1 \mu\text{m}$.

However, Zhu et al. [78] only added 3 wt.% Zn to the Sn-58Bi solder and found that it could refine the structure because the average intercept length of Bi-rich phase was smaller than that of the Sn-58Bi solder. Sukanuma et al. [79] pointed out that adding 0.5 wt.% and 1.0 wt.% Ag, respectively, to the Sn-58Bi solder alloy changed the microstructures. The size of particles in the Sn-57Bi-0.5Ag solder was less than $5 \mu\text{m}$, but the Ag_3Sn formed in the Sn-57Bi-1.0Ag solder appeared larger the size of which was larger than $10 \mu\text{m}$. Mokhtari and Nishikawa [64] have reported the

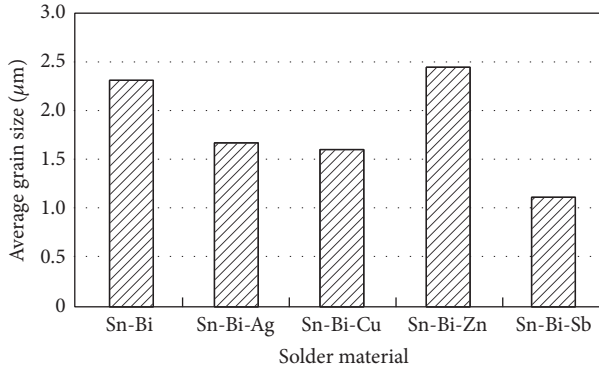


FIGURE 6: Comparison of average grain sizes of eutectic structures (Sn-Bi- x , $x = 0.5$ wt.% Ag, Cu, Zn, Sb) [65].

distinct analysis about the microstructures of soldered alloys bearing 0.5 wt.% In or Ni in Figure 7. Compared with the Sn-58Bi solder, the microstructure of Sn-Bi-0.5In solder exhibits a larger volume fraction of primary Sn dendrites, but adding Ni to Sn-58Bi solder can refine the microstructure. Compared to the Sn-57Bi solder, the grain size of the microstructure of the solder Sn-57Bi with the addition of 2.5% Fe ($\sim 2 \mu\text{m}$ in average diameter) dispersion is smaller [73].

The microstructures of the Sn-58Bi solders by adding 0.5 wt.% and 1 wt.% Cu_6Sn_5 reinforcement particles which were well dispersed in the solders matrix were refined and the grain size of β -Sn and Bi-rich phase was reduced [36]. Adding appropriate nanosized graphite could refine the microstructure of the composite solder [37].

The results indicated that, from the beginning, the microstructure of the solder with 0.07 wt.% nanosized graphite did not change greatly compared with that of the Sn-Bi matrix solder. But it was gradually refined with the nanosized graphite increased. When content of nanosized graphite is at 0.6 wt.%, the microstructure of composite solder was refined well. As can be seen in Table 3 [67], the addition of GNSs influenced extensively the interphase spacing of the primary phases of the Sn-58Bi0.7Zn solder. The interphase spacing was reduced by 12.92%, 32.52%, and 16.86%, respectively, with different addition of GNSs ranging from 0.038 wt.% to 0.114 wt.%. In addition, it was found that the effect of 0.076 wt.% GNSs was most perfect among the various contents.

Liu et al. [35] proposed that the microstructures of all composite solders with empty or different amounts of Y_2O_3 were coarsened after aging 550 h at 120°C , but the coarsening for the Sn-58Bi solder with 3.0 wt.% Y_2O_3 was the lowest. This indicated one thing that the addition of the Y_2O_3 could depress the coarsening rate during aging. Varying weight percentages of nanofillers Cu and Ni additions from 0 to 4.0 wt.% were incorporated [74]. Without nanofillers addition, the average interphase spacing of the Sn-58Bi solder was about $2.62 \mu\text{m}$. However, the size was decreased after the nanofillers Cu and Ni were added. It was noticed that the average interphase spacing of the Sn-58Bi solder with Cu addition was decreased from $1.73 \mu\text{m}$ to $1.21 \mu\text{m}$. The effect of

TABLE 3: Average interphase spacing in undoped and GNS-doped Sn-58Bi0.7Zn solders [67].

Solder	Interphase spacing (μm)
Sn-58Bi0.7Zn	0.527 ± 0.156
Sn-52Bi-0.7Zn0.038GNS	0.459 ± 0.123
Sn-52Bi-0.7Zn0.076GNS	0.355 ± 0.069
Sn-52Bi-0.7Zn0.114GNS	0.438 ± 0.095

nanofillers Ni addition on the microstructure of the Sn-58Bi solder was similar to the above results.

Shin et al. [50] added SiC nanoparticles (45–55 nm) to the Sn-58Bi solder. The mean size of lamellar structures of the Sn-58Bi solder was decreased from $1.97 \mu\text{m}$ to $1.32 \mu\text{m}$ by 32.9%. And the average size of lamellar structures reduced by 34.6% after 100 h aging. At the same time, after 400 h aging, the mean grain of the lamellar structures declined from $4.59 \mu\text{m}$ to $2.37 \mu\text{m}$. It could be seen that the SiC nanoparticles refine the microstructure of the Sn-58Bi solder.

Dong et al. [25] investigated that adding trace amounts of RE elements (primarily Ce and La) had better effect on refining the microstructure of the Sn-58Bi solder than that of the solder with 0.5 wt.% Ag addition. At the same time, the sizes of the Sn-rich phase in the condition of high-temperature aging were larger than that of solders in the as-reflowed state. According to EDS analysis results, it was assumed that many Bi-rich dendrites were distributed in the Sn-Bi-Ag solder alloy at the beginning and then the volume fraction of Bi-rich dendrites was reduced after adding minor RE to solder alloy. At the same time, the microstructures of them were refined particularly in SnBiAg-0.25RE and SnBiAg-0.5RE solder alloys [53]. Shiue and Chuang [52] only added La element to the Sn-58Bi solder to form a new type of solder, namely, Sn-58Bi-0.5La. They found many thin plate-shaped intermetallic compounds can be seen in the Sn-58Bi-0.5La.

7. Intermetallic Compounds Layer

Good bonding often depends on a thin, continuous, and uniform IMC layer [80]. At the interface, intermetallic compounds (IMCs) are formed as reaction products between solder and substrate during soldering which play a vital role in determining the long term reliability of microelectronic packages [81, 82]. The IMC nucleation, growth, and its type are responsible for the solder reliability [83, 84]. In addition, the IMC formed at first could function as a hard diffusion barrier to restrain further IMC growth [29]. At the same time, a part of Bi atoms dissolve into the Cu_6Sn_5 intermetallic compound layer and then segregate at the Cu/Cu₃Sn interface. It leads to weakening the copper/intermetallic interface and becoming the preferred fracture path after the above circumstances happen [85, 86].

Suganuma [87] also proposed that Cu_6Sn_5 and Cu_3Sn were formed at the interface between lead-free solder and Cu substrate. In addition, Shang et al. [88] observed interfacial voids near the Bi particles. Yoon et al. [89] also found that the thickness of the intermetallic compounds was increased with

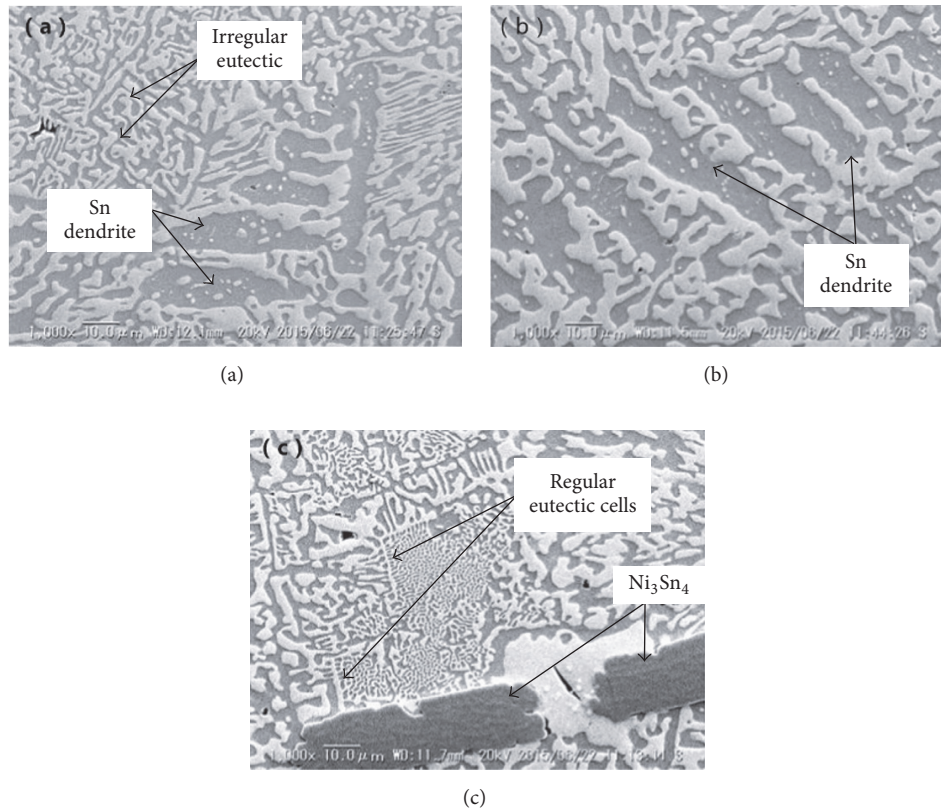


FIGURE 7: Microstructure of tensile samples: (a) eutectic Sn-Bi, (b) (Sn-Bi)-0.5In, and (c) (Sn-Bi)-0.5Ni [64].

aging time increased from 70 to 120°C. Now, as is known to us, adding very trace amounts of a few alloying elements to Sn-Bi solders can form a barrier layer that restrains the formation of the interfacial IMCs under high temperature state [90].

It was found that the addition of 0.1 wt.% Cu ameliorated remarkably in refinement of Bi-rich phase because Cu reacted with Sn to form Cu_6Sn_5 IMC particles [44] and Bi atoms dissolved in the Cu_6Sn_5 phase during the reflow process [91]. Different with Sn-40Bi-0.1Cu solder, Cu_6Sn_5 particles did not appear in Sn-40Bi-2Zn-0.1Cu solder which meant that all Cu content reacted with Zn to form Cu-Zn IMC because Cu has a higher affinity for reaction with Zn than Sn dose. When 1.0 wt.% Cu was added to the Sn-58Bi solder, the thickness of IMC for the Sn-58Bi-1Cu/PtAg/ Al_2O_3 joint was increased from 2.4 μm to 11 μm during aging time at 120°C lower than that for the Sn-58Bi/PtAg/ Al_2O_3 [40]. Li et al. [23] only found Ni_3Sn_4 in both the Sn-Bi/Ni and Sn-Bi/Ni-P systems, but the $(Cu, Ni)_6Sn_5$ replaced Ni_3Sn_4 after the addition of 1.0 wt.% Cu to the Sn-Bi solder due to the limit of lower solubility of Ni in the Cu_6Sn_5 with increasing reaction time. Zang et al. [31] revealed the composition of the IMC between the Sn-30Bi-0.5Cu solder and the Cu substrate. The double-layer IMCs consisting of Cu_6Sn_5 adjacent to the solder and Cu_3Sn adjacent to the copper substrate. Zhu et al. [78] studied that adding 3.0 wt.% Zn to the Sn-Bi solder could increase the average thickness of 41Sn-56Bi-3Zn composite solder to 10 μm and this IMC was further determined to be Cu_5Sn_8 phase which meant no Sn element and it was not

found that the Bi segregation during aging at 120°C for 7 days. Ma and Wu [45] also added Zn elements to the Sn-58Bi solder and a CuZn and $Cu_6(Sn, Zn)_5$ layer formed at the Cu/Sn-58Bi-0.7Zn interface during the soldering and the whole aging process. The thickness of the IMC layers between the Sn-58Bi-0.7Zn solder and Cu substrate changed like a parabolic law as the aging time increased from 1.8 μm to 5 μm . At the same time, Chen et al. [33] also studied the effect of Zn addition ranging from 2.0 wt.% to 4.0 wt.% on the thickness of reaction layers of Sn-42Bi alloy. The thickness of reaction layers was increased from 1.17 μm to 1.76 μm , but all lower than that of the Sn-42Bi alloy at 170°C. Similarly, at 190°C, the thickness of reaction layers grew from 1.34 μm to 1.81 μm lower that of 2.02 μm of the Sn-42Bi alloy. So the Zn addition decreased the thickness of reaction layers of the Sn-42Bi alloy. Kotadia et al. [90] detected that adding 1 wt.% Ag to Sn-Bi solder could reduce the consumption rate of the Cu substrate, because Ag_3Sn was formed and captured at the surface of the Cu_6Sn_5 grains reducing the interfacial energy which led to slowing down the IMC growth. Mokhtari and Nishikawa [59] reported that adding In or Ni element to the Sn-58Bi solder did not affect the thickness of the IMCs at the interface between the solder and the substrate before aging. But it exhibited differences from the Sn-58Bi solder after 6 weeks of aging and it was clear to be found that the IMC thickness of Sn-Bi-INi is thinner than others'. When these that were added 0.5 wt.% In and Ni are soldering, respectively, their IMC thicknesses were similar after 6 weeks of aging

TABLE 4: Total thickness of Sn-Bi-Sb/Cu reaction layers [32].

Alloy	Layer thickness/ μm
Sn-58Bi	2.34
Sn-52Bi-1.8Sb	2.43
Sn-48Bi-1.4Sb	2.43
Sn-48Bi-1.8Sb	2.51
Sn-48Bi-2.0Sb	2.76
Sn-48Bi-2.4Sb	2.85

and Sn-58Bi solder's IMC thickness increased as aging time increased. As Table 4 shows, it exhibited that the IMC layer thickness was gradually increased with increasing Sb content [32]. It was increased by 21.8% to 2.85 μm when Sb content was at 2.4 wt.%. The IMC layer thickness of Sn-52Bi-1.8Sb/Cu and Sn-48Bi-1.4Sb/Cu was the same 2.43 μm .

Li et al. [92] found that the additions of 1-2 wt.% Al, Cr, Si, Nb, Pt, and Cu had no obvious effect on the IMC growth of the Sn-58Bi/Cu not slowing down IMC growth at both 200 and 240°C. But it could be observed that Al accumulated and oxidized at the surface of the Sn-56.8Bi-2Al solder during high-temperature storage. It was shown that no Cr, Si, and Nb were detected almost due to low solubility in the Sn-58Bi solder. The addition of 1 wt.% Cu also had no effect on the IMC growth. Li et al. [29] added 1.0 wt.% Au and Zn to the Sn-58Bi solder and found that the growth rate of the IMCs of the composite solders was increased. In contrast, addition of the 2 wt.% Cr, 2 wt.% Si, and 1 wt.% Ag elements reduced the growth rate and did not affect critically the interfacial microstructures at 200°C and 240°C for 120 h.

Huang and Chen [49] studied adding Co element to Sn-57Bi solder. The results were plotted in Figure 8. Only one product was found and it was Cu_6Sn_5 . After reacting for 10 min, it was seen that the thickness of Sn-57Bi was increased after added Co element and the IMC thickness of Sn-57Bi-0.5Co was highest. Similarly, after reacting for 4 h, the IMC thickness of the three solders/Cu was all increased.

Figure 9 implied the relationship between the IMC layer thicknesses of Sn-Bi/Cu, Sn-Bi-0.05Co, and Sn-57Bi-(Co)/Cu couples aged at 100°C. It could be referred to as a diffusion control kinetics. The growth rate of all solders was like parabolic curve. As could be seen from the picture, the reaction layer was thicker with greater Co addition.

Hu et al. [62] adding 0.5 wt.% Al_2O_3 nanoparticles to the Sn-58Bi solder have found that the average thickness of the IMC layer of the composite solder was declined from 2.5 μm to 1.27 μm compared with that of Sn-58Bi experiencing 288 aging hours at 85°C. Cu_6Sn_5 was observed to form the IMC by using XRD and it was assumed that these Cu_6Sn_5 grain size was decreased with the addition of Y_2O_3 increased [35]. Y_2O_3 ranging from 0.5 wt.% to 3.0 wt.% could restrain the grain division between IMC particles decreasing the surface energy of the compounds and limited the growth of the IMC. So the thickness of IMC layer of the Sn-58Bi solder with the addition of Y_2O_3 was thinner than that of the Sn-58Bi solder. Shin et al. [50] found that the thickness of the intermetallic compounds of the Sn-58Bi solder changed slightly after the

SiC nanoparticles were added to the Sn-58Bi solder during different aging time at 100°C. The thickness of the IMC layer of Sn-Bi/Cu and Sn-Bi-SiC/Cu was increased from 0.75 μm to 2.3 μm with aging time increased. After aging of 100 h, the thickness of the IMC layers of the Sn-58Bi and Sn-58Bi-SiC solder was almost the same. After 400 h aging time, the thickness of the IMC layer of the Sn-58Bi solder was higher. Liu et al. [36] added Cu_6Sn_5 particles to the Sn-58Bi solder. At the beginning, it was found large Cu_6Sn_5 particles on the top of IMC grain of SB-1 $\text{Cu}_6\text{Sn}_5/\text{Cu}$ due to the gravity. But as the soldering time increased, the larger Cu_6Sn_5 was incorporated into the smaller ones to form scallop-shaped Cu_6Sn_5 compounds in a mature process. Last, the grain size of IMC increased because of the decreasing dissolution rate of the IMC compared with Sn-58Bi/Cu. Ma and Wu [67] investigated the effect of addition of GNSs on the IMC layers of the Sn-58Bi-0.7Zn which reacted with Cu substrate during liquid-state aging at 150°C for different time (20, 40, 60, 80, 100, and 120 min). The thickness of the four types of solders was 1.56, 1.32, 1.05, and 0.87 μm , respectively, after 20 min aging time. It was seen that with the increasing GNSs addition the thickness was decreased. However, the thickness of the four types of solders was increased as the liquid-state aging times added up to 6.50, 4.77, 3.63, and 2.75 μm . Shiue and Chuang [52] demonstrated that the thickness of the Sn-58Bi solders with 0.5 wt.% La element was thinner than that of those Sn-58Bi after aging at 75 and 100°C for various aging times. At 75°C, the IMC layer thickness of the two Sn-58Bi and Sn-58Bi-La solder was increased from 1.4 μm and 0.8 μm to 2.25 μm and 1.25 μm as aging time increased. However, it was clear to see that the thickness of IMC layer of the Sn-58Bi solder was higher than the later. At the same time, the IMC layer thickness of the Sn-58Bi solder was increased critically by 124.8% from 1.49 μm to 3.35 μm and it was higher than that of the Sn-58Bi-0.5La at 100°C for various aging times.

As could be seen from Figure 10, Dong et al. [25] studied the effects of the addition of 0.1 wt.% RE elements (primarily Ce and La) and 0.5 wt.% Ag on the average thickness of IMC of the Sn-58Bi/Cu. At the beginning, all solders were reflowed. It was found that only the thickness of the IMC of Sn-58Bi-0.5Ag was increased by 31.4% from 1.75 μm to 2.3 μm . After aging of 168 hours at 80°C, the changes were great. It was appreciable to be seen that the thickness of IMC was increased critically in addition to the Sn-58Bi-0.1RE solder after high-temperature aging. Because the RE elements could improve chemical reactions at the interface and provide very strong bonding during soldering, the increase of the IMC thickness of the Sn-58Bi-0.5Ag-0.1RE solder after aging was less than that of the Sn-58Bi-0.5Ag solder. The reasons for this may be the fact that RE elements have a stronger affinity for oxygen than most metals and tend to reduce metal oxides. So it can be found that the addition of 0.5 wt.% Ag promoted the IMC thickness remarkably by 121% from 2.3 μm to 5.1 μm .

Wu et al. [53] found that there were Bi-rich dendrites, Ag_3Sn , and RE (Bi, Sn)₃ close to the Cu_6Sn_5 IMC layer by observing the SEM images of the interfacial microstructures of the as-reflowed Sn-Bi-Ag/Cu and Sn-Bi-Ag-xRE/Cu solder joints. As the addition of RE increased, Cu_6Sn_5 at the interface of Sn-Bi-Ag-xRE/Cu solder joints was refined and

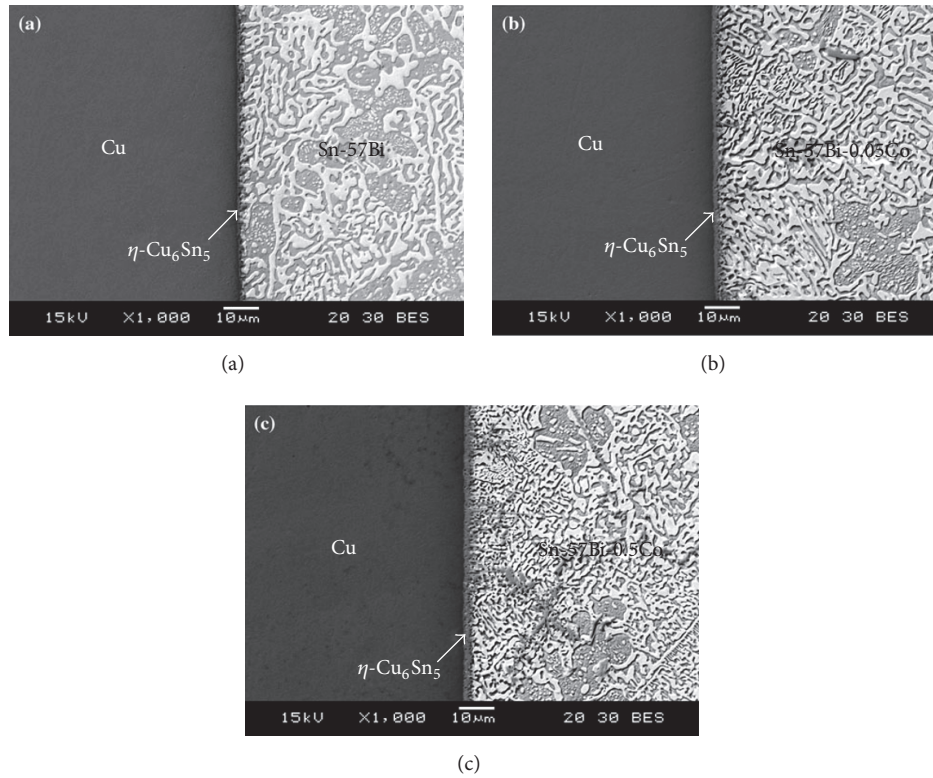


FIGURE 8: BEI micrographs of large reaction couples reacted at 160°C for 10 min: (a) Sn-57 wt.% Bi/Cu, (b) Sn-57 wt.% Bi-0.05 wt.% Co/Cu, and (c) Sn-57 wt.% Bi-0.5 wt.% Co/Cu [49].

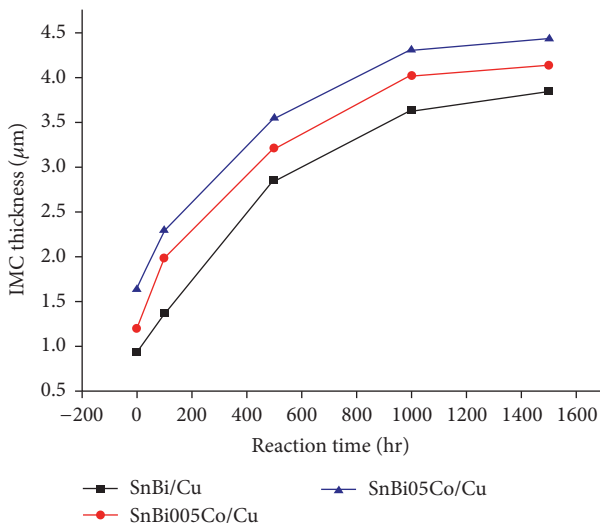


FIGURE 9: Relationship between total IMC layer thickness and aging time at 100°C [49].

the thickness of IMC layer was thinner than others when the content of RE addition at 0.25%.

8. Reliability

In electronic package, the major cause for failure of electronic devices is thermal fatigue accounting for 55% when semicon-

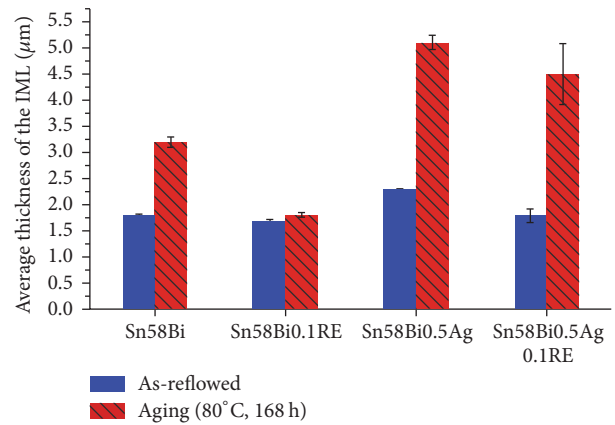


FIGURE 10: Average thickness of the IMC at the solder/Cu interface [25].

ductor packages are exposed to various environments such as temperature, humidity, dust, shock, and vibration [54]. During thermal cycling, solder joints are prone to failures although they provide reliable bonding between the package and the board in the electrical devices [93]. At the same time, Liu and Shang [94] found that aging promoted Bi segregation to the Cu-intermetallic interface resulting in a sharp decrease in fatigue and fracture resistance of the interface.

The fatigue life of the Sn-58Bi, Sn-35Bi-0.3Ag, and Sn-35Bi-1.0Ag was studied by Zhang et al. [34]. The results

exhibited that the fatigue life of the Sn-35Bi solder with 0.5 wt.% and 1.0 wt.% Ag was increased by 13.75% and 20%, respectively, compared with that of the Sn-58Bi solder. At the same time, some researchers also investigated the effect of Ag addition on the thermal fatigue life of the Sn-58Bi solder. All solder joints including Sn-58Bi, Sn-37Pb, and Sn-58Bi-2Ag solder joints experienced the temperature profile which was $-20^{\circ}\text{C}\leftrightarrow 100^{\circ}\text{C}$ with an hour per cycle and a dwell time of 10 min at the low and high temperatures. Sn-37Pb lasted longer than Sn-58Bi. The fatigue life of Sn-58Bi solder with 2 wt.% Ag addition was increased critically and it was longer than fatigue life of Sn-58Bi and Sn-37Pb solders at the beginning [95]. With the cyclic strain increased, however, the fatigue lives of these solder joints were decreased.

9. Conclusions

As can be seen from the above, the properties of the Sn-Bi solders, such as wettability, melting behavior, and mechanical properties, and solder joints were improved extensively due to the addition of alloying elements. For example, the mean tensile strength was increased by 12.6% after adding 0.1 wt.% Cu to Sn-40Bi solder. The effects of RE addition on the microstructure of Sn-Bi solders were obvious because of its higher activity. Nanoparticles were often added to strengthen the properties and solder joints. However, the properties were also decreased for excessive elements. For example, the UTS of the Sn-58Bi- x Zn was firstly increased and then decreased with the increasing addition of Zn element [45]. So it is critical to select appropriate amount of these additives. Adding nanoparticles and RE elements did not change greatly the melting temperatures of Sn-Bi solders. Whereas it is found that the effects of nanoparticles additions on the microstructures of Sn-Bi solders are obvious and adding minor alloy elements can depress the intermetallic thickness.

Competing Interests

The authors declare that they have no conflict of interests.

Acknowledgments

This study was funded by the Research Innovation Project for College Graduate of Jiangsu Province (KYZZ16_0469), the Natural Science Foundation of China (51475220), the State Foundation of Laboratory of Advanced Brazing Filler Metals & Technology (Zhengzhou Research Institute of Mechanical Engineering) (SKLABFMT-2015-03), Six Kind Skilled Personnel Project of Jiangsu Province (XCL-022), the Qing Lan Project and High Level Talent Plan of Jiangsu Normal University (YQ2015002). Liang Zhang and Fan Yang have received research grants from Jiangsu Normal University.

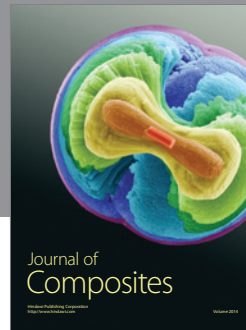
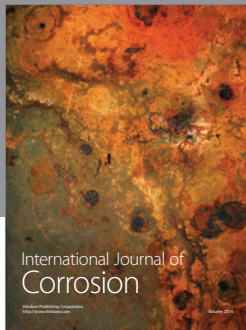
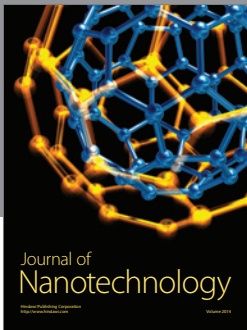
References

- [1] J. Li, Z. Yuan, Z. Qiao, J. Fan, Y. Xu, and J. Ke, "Measurement and calculation of surface tension of molten Sn-Bi alloy," *Journal of Colloid and Interface Science*, vol. 297, no. 1, pp. 261–265, 2006.
- [2] L. Zhang and K. N. Tu, "Structure and properties of lead-free solders bearing micro and nano particles," *Materials Science & Engineering R: Reports*, vol. 82, no. 1, pp. 1–32, 2014.
- [3] D. Q. Yu, J. Zhao, and L. Wang, "Improvement on the microstructure stability, mechanical and wetting properties of Sn-Ag-Cu lead-free solder with the addition of rare earth elements," *Journal of Alloys & Compounds*, vol. 376, no. 1–2, pp. 170–175, 2004.
- [4] S. Nurmi, J. Sundelin, E. Ristolainen, and T. Lepistö, "The effect of solder paste composition on the reliability of SnAgCu joints," *Microelectronics Reliability*, vol. 44, no. 3, pp. 485–494, 2004.
- [5] L. Zhang, S. Xue, Y. Chen et al., "Effects of cerium on Sn-Ag-Cu alloys based on finite element simulation and experiments," *Journal of Rare Earths*, vol. 27, no. 1, pp. 138–144, 2009.
- [6] S. F. Choudhury and L. Ladani, "Local shear stress-strain response of Sn-3.5Ag/Cu solder joint with high fraction of intermetallic compounds: experimental analysis," *Journal of Alloys & Compounds*, vol. 680, pp. 665–676, 2016.
- [7] Y. Yao, J. Zhou, F. Xue, and X. Chen, "Interfacial structure and growth kinetics of intermetallic compounds between Sn-3.5Ag solder and Al substrate during solder process," *Journal of Alloys and Compounds*, vol. 682, pp. 627–633, 2016.
- [8] J. Liu, Z. Wang, J. Xie et al., "Effects of intermetallic-forming element additions on microstructure and corrosion behavior of Sn-Zn solder alloys," *Corrosion Science*, vol. 112, pp. 150–159, 2016.
- [9] W. Xing, X. Yu, H. Li et al., "Microstructure and mechanical properties of Sn-9Zn-xAl₂O₃ nanoparticles (x=0–1) lead-free solder alloy: first-principles calculation and experimental research," *Materials Science and Engineering: A*, vol. 678, pp. 252–259, 2016.
- [10] B. L. Silva, G. Reinhart, H. Nguyen-Thi, N. Manginck-Noël, A. Garcia, and J. E. Spinelli, "Microstructural development and mechanical properties of a near-eutectic directionally solidified Sn-Bi solder alloy," *Materials Characterization*, vol. 107, pp. 43–53, 2015.
- [11] O. Mokhtari and H. Nishikawa, "The shear strength of transient liquid phase bonded Sn-Bi solder joint with added Cu particles," *Advanced Powder Technology*, vol. 27, no. 3, pp. 1000–1005, 2016.
- [12] B. L. Silva, N. Cheung, A. Garcia, and J. E. Spinelli, "Evaluation of solder/substrate thermal conductance and wetting angle of Sn-0.7 wt%Cu-(0–0.1 wt%Ni) solder alloys," *Materials Letters*, vol. 142, pp. 163–167, 2015.
- [13] T. Maeshima, H. Ikehata, K. Terui, and Y. Sakamoto, "Effect of Ni to the Cu substrate on the interfacial reaction with Sn-Cu solder," *Materials & Design*, vol. 103, pp. 106–113, 2016.
- [14] M. Yang, H. Ji, S. Wang et al., "Effects of Ag content on the interfacial reactions between liquid Sn-Ag-Cu solders and Cu substrates during soldering," *Journal of Alloys & Compounds*, vol. 679, pp. 18–25, 2016.
- [15] D. Giuranno, S. Delsante, G. Borzone, and R. Novakovic, "Effects of Sb addition on the properties of Sn-Ag-Cu/(Cu, Ni) solder systems," *Journal of Alloys and Compounds*, vol. 689, pp. 918–930, 2016.
- [16] M. Mostofizadeh, J. Pippola, T. Marttila, and L. Frisk, "Effect of isothermal aging and salt spray tests on reliability and mechanical strength of eutectic Sn-Bi lead-free solder joints," in *Proceedings of the 13th International Thermal, Mechanical and Multi-Physics Simulation and Experiments in Microelectronics and Microsystems (EuroSimE '12)*, April 2012.

- [17] Y. Goh, A. S. M. A. Haseeb, and M. F. M. Sabri, "Effects of hydroquinone and gelatin on the electrodeposition of Sn-Bi low temperature Pb-free solder," *Electrochimica Acta*, vol. 90, pp. 265–273, 2013.
- [18] S. F. Lee, Y. Goh, and A. S. M. A. Haseeb, "Effects of stacking sequence of electrodeposited Sn and Bi layers on reflowed Sn-Bi solder alloys," in *Proceedings of the 35th IEEE/CPMT International Electronics Manufacturing Technology Conference (IEMT '12)*, 6, 1 pages, Perak, Malaysia, November 2012.
- [19] J. H. Wang, L. Wen, J. W. Zhou, and M. Chung, "Mechanical properties and joint reliability improvement of Sn-Bi alloy," in *Proceedings of the IEEE 13th Electronics Packaging Technology Conference (EPTC '11)*, pp. 492–496, Singapore, December 2011.
- [20] M.-H. Roh, J. P. Jung, and W. Kim, "Microstructure, shear strength, and nanoindentation property of electroplated Sn-Bi micro-bumps," *Microelectronics Reliability*, vol. 54, no. 1, pp. 265–271, 2014.
- [21] P. T. Vianco, A. C. Kilgo, and R. Grant, "Intermetallic compound layer growth by solid state reactions between 58Bi-42Sn solder and copper," *Journal of Electronic Materials*, vol. 24, no. 10, pp. 1493–1505, 1995.
- [22] M. Kitajima and T. Shono, "Reliability study of new SnZnAl lead-free solders used in CSP packages," *Microelectronics Reliability*, vol. 45, no. 7-8, pp. 1208–1214, 2005.
- [23] J. F. Li, S. H. Mannan, M. P. Clode et al., "Comparison of interfacial reactions of Ni and Ni-P in extended contact with liquid Sn-Bi-based solders," *Acta Materialia*, vol. 55, no. 2, pp. 737–752, 2007.
- [24] X. Chen, F. Xue, J. Zhou, and Y. Yao, "Effect of in on microstructure, thermodynamic characteristic and mechanical properties of Sn-Bi based lead-free solder," *Journal of Alloys & Compounds*, vol. 633, pp. 377–383, 2015.
- [25] W. Dong, Y. Shi, Z. Xia, Y. Lei, and F. Guo, "Effects of trace amounts of rare earth additions on microstructure and properties of Sn-Bi-based solder alloy," *Journal of Electronic Materials*, vol. 37, no. 7, pp. 982–991, 2008.
- [26] L. Sun and L. Zhang, "Properties and microstructures of Sn-Ag-Cu-X lead-free solder joints in electronic packaging," *Advances in Materials Science and Engineering*, vol. 2015, Article ID 639028, 16 pages, 2015.
- [27] E. E. M. Noor, N. M. Sharif, C. K. Yew, T. Ariga, A. B. Ismail, and Z. Hussain, "Wettability and strength of In-Bi-Sn lead-free solder alloy on copper substrate," *Journal of Alloys and Compounds*, vol. 507, no. 1, pp. 290–296, 2010.
- [28] J. W. Morris Jr., J. L. F. Goldstein, and Z. Mei, "Microstructure and mechanical properties of Sn-In and Sn-Bi solders," *JOM*, vol. 45, no. 7, pp. 25–27, 1993.
- [29] J. F. Li, S. H. Mannan, M. P. Clode et al., "Interactions between liquid Sn-Bi based solders and contact metals for high temperature applications," in *Proceedings of the 55th Electronic Components and Technology Conference (ECTC '05)*, pp. 441–448, Lake Buena Vista, Fla, USA, June 2005.
- [30] H.-W. Miao, J.-G. Duh, and B.-S. Chiou, "Thermal cycling test in Sn-Bi and Sn-Bi-Cu solder joints," *Journal of Materials Science: Materials in Electronics*, vol. 11, no. 8, pp. 609–618, 2000.
- [31] L. Zang, Z. Yuan, H. Zhao, and X. Zhang, "Wettability of molten Sn-Bi-Cu solder on Cu substrate," *Materials Letters*, vol. 63, no. 23, pp. 2067–2069, 2009.
- [32] C. Zhang, S.-D. Liu, G.-T. Qian, J. Zhou, and F. Xue, "Effect of Sb content on properties of Sn-Bi solders," *Transactions of Nonferrous Metals Society of China (English Edition)*, vol. 24, no. 1, pp. 184–191, 2014.
- [33] X. Chen, F. Xue, J. Zhou, S. Liu, and G. Qian, "Microstructure, thermal and wetting properties of Sn-Bi-Zn lead-free solder," *Journal of Electronic Materials*, vol. 42, no. 8, pp. 2708–2715, 2013.
- [34] L. Zhang, L. Sun, and Y.-H. Guo, "Microstructures and properties of Sn₅₈Bi, Sn₃₅Bi_{0.3}Ag, Sn₃₅Bi_{1.0}Ag solder and solder joints," *Journal of Materials Science: Materials in Electronics*, vol. 26, no. 10, pp. 7629–7634, 2015.
- [35] X. Liu, M. Huang, C. M. L. Wu, and L. Wang, "Effect of Y₂O₃ particles on microstructure formation and shear properties of Sn-58Bi solder," *Journal of Materials Science: Materials in Electronics*, vol. 21, no. 10, pp. 1046–1054, 2010.
- [36] X. Liu, M. Huang, and N. Zhao, "Effect of Cu₆Sn₅ particles on microstructure formation and mechanical properties of Sn-58Bi solder," in *Proceedings of the 13th International Conference on Electronic Packaging Technology and High Density Packaging (ICEPT-HDP '12)*, pp. 423–425, Guilin, China, August 2012.
- [37] L. Yang, C. Du, J. Dai, N. Zhang, and Y. Jing, "Effect of nanosized graphite on properties of Sn-Bi solder," *Journal of Materials Science: Materials in Electronics*, vol. 24, no. 11, pp. 4180–4185, 2013.
- [38] B. Brunetti, D. Gozzi, M. Iervolino et al., "Bismuth activity in lead-free solder Bi-In-Sn alloys," *Calphad: Computer Coupling of Phase Diagrams & Thermochemistry*, vol. 30, no. 4, pp. 431–442, 2006.
- [39] S. H. Mannan, M. P. Clode, and M. Dagher, "Study of intermetallic crystal growth between Nb and molten 52In-48Sn solder," *Journal of Electronic Materials*, vol. 34, no. 2, pp. 125–131, 2005.
- [40] H.-W. Miao and J.-G. Duh, "Microstructure evolution in Sn-Bi and Sn-Bi-Cu solder joints under thermal aging," *Materials Chemistry and Physics*, vol. 71, no. 3, pp. 255–271, 2001.
- [41] C.-H. Yeh, L.-S. Chang, and B. B. Straumal, "Wetting transition of grain boundaries in the Sn-rich part of the Sn-Bi phase diagram," *Journal of Materials Science*, vol. 46, no. 5, pp. 1557–1562, 2011.
- [42] Z. Guo, W. Yuan, M. Hindler, and A. Mikula, "Thermodynamic properties of liquid Au-Bi-Sn alloys," *Journal of Chemical Thermodynamics*, vol. 48, pp. 201–206, 2012.
- [43] I. Shafiq, Y. C. Chan, S. Xu, and Q. Q. Li, "Electro-migration study of nano Al doped lead-free Sn-58Bi on Cu and Au/Ni/Cu ball grid array (BGA) packages," in *Proceedings of the 18th European Microelectronics and Packaging Conference (EMPC '11)*, pp. 1–7, Brighton, UK, 2011.
- [44] J. Shen, Y. Pu, H. Yin, D. Luo, and J. Chen, "Effects of minor Cu and Zn additions on the thermal, microstructure and tensile properties of Sn-Bi-based solder alloys," *Journal of Alloys & Compounds*, vol. 614, pp. 63–70, 2014.
- [45] D.-L. Ma and P. Wu, "Effects of Zn addition on mechanical properties of eutectic Sn-58Bi solder during liquid-state aging," *Transactions of Nonferrous Metals Society of China (English Edition)*, vol. 25, no. 4, article 63719, pp. 1225–1233, 2015.
- [46] Y. Altıntaş, Y. Kaygıslı, E. Öztürk, S. Aksöz, K. Keşlioğlu, and N. Maraşlı, "The measurements of electrical and thermal conductivity variations with temperature and phonon component of the thermal conductivity in Sn-Cd-Sb, Sn-In-Cu, Sn-Ag-Bi and Sn-Bi-Zn alloys," *International Journal of Thermal Sciences*, vol. 100, pp. 1–9, 2016.
- [47] S.-K. Lin, T. L. Nguyen, S.-C. Wu, and Y.-H. Wang, "Effective suppression of interfacial intermetallic compound growth between Sn-58 wt.% Bi solders and Cu substrates by minor Ga

- addition," *Journal of Alloys & Compounds*, vol. 586, no. 4, pp. 319–327, 2014.
- [48] R. M. Shalaby, "Effect of silver and indium addition on mechanical properties and indentation creep behavior of rapidly solidified Bi-Sn based lead-free solder alloys," *Materials Science and Engineering A*, vol. 560, pp. 86–95, 2013.
- [49] Y.-C. Huang and S.-W. Chen, "Effects of Co alloying and size on solidification and interfacial reactions in Sn-57 wt.%Bi-(Co)/Cu couples," *Journal of Electronic Materials*, vol. 40, no. 1, pp. 62–70, 2011.
- [50] Y. S. Shin, S. Lee, S. Yoo, and C. W. Lee, "Mechanical and microstructural properties of SiC-mixed Sn-Bi composite solder bumps by electroplating," in *Proceedings of the European Microelectronics and Packaging Conference (EMPC '09)*, June 2009.
- [51] Y. Peng and K. Deng, "Fabrication of reduced graphene oxide nanosheets reinforced Sn-Bi nanocomposites by electrochemical deposition," *Composites Part A: Applied Science and Manufacturing*, vol. 73, pp. 55–62, 2015.
- [52] Y.-Y. Shiue and T.-H. Chuang, "Effect of La addition on the interfacial intermetallics and bonding strengths of Sn-58Bi solder joints with Au/Ni/Cu pads," *Journal of Alloys & Compounds*, vol. 491, no. 1-2, pp. 610–617, 2010.
- [53] C. Wu, J. Shen, and C. Peng, "Effects of trace amounts of rare earth additions on the microstructures and interfacial reactions of Sn57Bi1Ag/Cu solder joints," *Journal of Materials Science: Materials in Electronics*, vol. 23, no. 1, pp. 14–21, 2012.
- [54] L. Zhang, C.-W. He, Y.-H. Guo, J.-G. Han, Y.-W. Zhang, and X.-Y. Wang, "Development of SnAg-based lead free solders in electronics packaging," *Microelectronics Reliability*, vol. 52, no. 3, pp. 559–578, 2012.
- [55] J. S. Zhang, Y. C. Chan, Y. P. Wu, H. J. Xi, and F. S. Wu, "Electromigration of Pb-free solder under a low level of current density," *Journal of Alloys & Compounds*, vol. 458, no. 1-2, pp. 492–499, 2008.
- [56] C.-M. Chen, Y.-M. Hung, and C.-H. Lin, "Electromigration of Sn-8 wt.% Zn-3 wt.% Bi and Sn-9 wt.% Zn-1 wt.% Cu solders," *Journal of Alloys & Compounds*, vol. 475, no. 1-2, pp. 238–244, 2009.
- [57] H. He, H. Zhao, F. Guo, and G. Xu, "Bi layer formation at the anode interface in Cu/Sn-58Bi/Cu solder joints with high current density," *Journal of Materials Science & Technology*, vol. 28, no. 1, pp. 46–52, 2012.
- [58] D. Ma and P. Wu, "Effects of coupled stressing and solid-state aging on the mechanical properties of Sn-58Bi-0.7Zn solder joint," *Journal of Materials Science: Materials in Electronics*, vol. 26, no. 8, pp. 6285–6292, 2015.
- [59] O. Mokhtari and H. Nishikawa, "Coarsening of Bi phase and intermetallic layer thickness in Sn-58Bi-X (X=In and Ni) solder joint," in *Proceedings of the 14th International Conference on Electronic Packaging Technology (ICEPT '13)*, vol. 15, pp. 250–253, Dalian, China, August 2013.
- [60] L.-T. Chen and C.-M. Chen, "Electromigration study in the eutectic SnBi solder joint on the Ni/Au metallization," *Journal of Materials Research*, vol. 21, no. 4, pp. 962–969, 2006.
- [61] C.-M. Chen and C.-C. Huang, "Effects of silver doping on electromigration of eutectic SnBi solder," *Journal of Alloys and Compounds*, vol. 461, no. 1-2, pp. 235–241, 2008.
- [62] T. Hu, Y. Li, Y.-C. Chan, and F. Wu, "Effect of nano Al₂O₃ particles doping on electromigration and mechanical properties of Sn-58Bi solder joints," *Microelectronics Reliability*, vol. 55, no. 8, pp. 1226–1233, 2015.
- [63] J. Glazer, "Microstructure and mechanical properties of Pb-free solder alloys for low-cost electronic assembly: a review," *Journal of Electronic Materials*, vol. 23, no. 8, pp. 693–700, 1994.
- [64] O. Mokhtari and H. Nishikawa, "Correlation between microstructure and mechanical properties of Sn-Bi-X solders," *Materials Science and Engineering A*, vol. 651, pp. 831–839, 2016.
- [65] S. Sakuyama, T. Akamatsu, K. Uenishi, and T. Sato, "Effects of a third element on microstructure and mechanical properties of eutectic Sn-Bi solder," *Transactions of the Japan Institute of Electronics Packaging*, vol. 2, no. 1, pp. 98–103, 2009.
- [66] Y. Kubota, I. Shohji, T. Tsuchida, and K. Nakamura, "Tensile properties of low-melting point Sn-Bi-Sb solder," in *Proceedings of the 16th IEEE Electronics Packaging Technology Conference (EPTC '14)*, December 2014.
- [67] D. L. Ma and P. Wu, "Improved microstructure and mechanical properties for Sn58Bi0.7Zn solder joint by addition of graphene nanosheets," *Journal of Alloys and Compounds*, no. 671, pp. 127–136, 2016.
- [68] P. He, X.-C. Lü, T.-S. Lin et al., "Improvement of mechanical properties of Sn-58Bi alloy with multi-walled carbon nanotubes," *Transactions of Nonferrous Metals Society of China*, vol. 22, supplement 3, pp. s692–s696, 2012.
- [69] Y. Peng and K. Deng, "Study on the mechanical properties of the novel Sn-Bi/Graphene nanocomposite by finite element simulation," *Journal of Alloys & Compounds*, vol. 625, no. 1, pp. 44–51, 2015.
- [70] L. Gao, S. Xue, L. Zhang, Z. Sheng, G. Zeng, and F. Ji, "Effects of trace rare earth Nd addition on microstructure and properties of SnAgCu solder," *Journal of Materials Science: Materials in Electronics*, vol. 21, no. 7, pp. 643–648, 2010.
- [71] D. Hou, D. Li, L. Han, and L. Ji, "Effect of lanthanum addition on microstructure and corrosion behavior of Al-Sn-Bi anodes," *Journal of Rare Earths*, vol. 29, no. 2, pp. 129–132, 2011.
- [72] L. Shen, P. Septiwerdani, and Z. Chen, "Elastic modulus, hardness and creep performance of SnBi alloys using nanoindentation," *Materials Science and Engineering A*, vol. 558, pp. 253–258, 2012.
- [73] S. Jin and M. McCormack, "Dispersoid additions to a Pb-free solder for suppression of microstructural coarsening," *Journal of Electronic Materials*, vol. 23, no. 8, pp. 735–739, 1994.
- [74] L. Shen, Z. Y. Tan, and Z. Chen, "Nanoindentation study on the creep resistance of SnBi solder alloy with reactive nano-metallic fillers," *Materials Science & Engineering: A*, vol. 561, no. 3, pp. 232–238, 2013.
- [75] C. H. Raeder, L. E. Felton, V. A. Tanzi, and D. B. Knorr, "The effect of aging on microstructure, room temperature deformation, and fracture of Sn-Bi/Cu solder joints," *Journal of Electronic Materials*, vol. 23, no. 7, pp. 611–617, 1994.
- [76] C. Niu, C. Li, Z. Du, C. Guo, and S. Chen, "A thermodynamic assessment of the Bi-Mg-Sn ternary system," *Calphad: Computer Coupling of Phase Diagrams and Thermochemistry*, vol. 39, pp. 37–46, 2012.
- [77] C. H. Raeder, L. E. Felton, D. B. Knorr, G. B. Schmeelk, and D. Lee, "Microstructural evolution and mechanical properties of Sn-Bi based solders," in *Proceedings of the 15th IEEE/CHMT International Electronics Manufacturing Technology (IEMT) Symposium*, pp. 119–127, October 1993.
- [78] Q. S. Zhu, H. Y. Song, H. Y. Liu, Z. G. Wang, and J. K. Shang, "Effect of Zn addition on microstructure of Sn-Bi joint," in *Proceedings of the International Conference on Electronic Packaging Technology and High Density Packaging (ICEPT-HDP '09)*, pp. 1043–1046, August 2009.

- [79] K. Sukanuma, T. Sakai, K.-S. Kim, Y. Takagi, J. Sugimoto, and M. Ueshima, "Thermal and mechanical stability of soldering QFP with Sn-Bi-Ag lead-free alloy," *IEEE Transactions on Electronics Packaging Manufacturing*, vol. 25, no. 4, pp. 257–261, 2002.
- [80] P. J. Shang, Z. Q. Liu, D. X. Li, and J. K. Shang, "TEM observations of the growth of intermetallic compounds at the SnBi/Cu interface," *Journal of Electronic Materials*, vol. 38, no. 12, pp. 2579–2584, 2009.
- [81] G. K. Sujana, A. S. M. A. Haseeb, and A. B. M. Afifi, "Effects of metallic nanoparticle doped flux on the interfacial intermetallic compounds between lead-free solder ball and copper substrate," *Materials Characterization*, vol. 97, pp. 199–209, 2014.
- [82] S. C. Yang, C. E. Ho, C. W. Chang, and C. R. Kao, "Massive spalling of intermetallic compounds in solder-substrate reactions due to limited supply of the active element," *Journal of Applied Physics*, vol. 101, no. 8, Article ID 084911, pp. 1–6, 2007.
- [83] Y. Takaku, X. J. Liu, I. Ohnuma, R. Kainuma, and K. Ishida, "Interfacial reaction and morphology between molten Sn base solders and Cu substrate," *Materials Transactions*, vol. 45, no. 3, pp. 646–651, 2004.
- [84] H. R. Kotadia, A. Panneerselvam, O. Mokhtari, M. A. Green, and S. H. Mannan, "Massive spalling of Cu-Zn and Cu-Al intermetallic compounds at the interface between solders and Cu substrate during liquid state reaction," *Journal of Applied Physics*, vol. 111, no. 7, Article ID 074902, 2012.
- [85] H. F. Zou, Q. K. Zhang, and Z. F. Zhang, "Eliminating interfacial segregation and embrittlement of bismuth in SnBi/Cu joint by alloying Cu substrate," *Scripta Materialia*, vol. 61, no. 3, pp. 308–311, 2009.
- [86] P. L. Liu and J. K. Shang, "Interfacial segregation of bismuth in copper/tin-bismuth solder interconnect," *Scripta Materialia*, vol. 44, no. 7, pp. 1019–1023, 2001.
- [87] K. Sukanuma, "Advances in lead-free electronics soldering," *Current Opinion in Solid State & Materials Science*, vol. 5, no. 1, pp. 55–64, 2001.
- [88] P. J. Shang, Z. Q. Liu, D. X. Li, and J. K. Shang, "Bi-induced voids at the Cu₃Sn/Cu interface in eutectic SnBi/Cu solder joints," *Scripta Materialia*, vol. 58, no. 5, pp. 409–412, 2008.
- [89] J.-W. Yoon, C.-B. Lee, and S.-B. Jung, "Interfacial reactions between Sn-58 mass% Bi eutectic solder and (Cu, electroless Ni-P/Cu) substrate," *Materials Transactions*, vol. 43, no. 8, pp. 1821–1826, 2002.
- [90] H. R. Kotadia, P. D. Howes, and S. H. Mannan, "A review: on the development of low melting temperature Pb-free solders," *Microelectronics Reliability*, vol. 54, no. 6-7, pp. 1253–1273, 2014.
- [91] Q. K. Zhang, H. F. Zou, and Z. F. Zhang, "Influences of substrate alloying and reflow temperature on Bi segregation behaviors at Sn-Bi/Cu interface," *Journal of Electronic Materials*, vol. 40, article 2320, 2011.
- [92] J. F. Li, S. H. Mannan, M. P. Clode, D. C. Whalley, and D. A. Hutt, "Interfacial reactions between molten Sn-Bi-X solders and Cu substrates for liquid solder interconnects," *Acta Materialia*, vol. 54, no. 11, pp. 2907–2922, 2006.
- [93] A. Schubert, R. Dudek, H. Walter et al., "Reliability assessment of flip-chip assemblies with lead-free solder joints," in *Proceedings of the 52nd Electronic Components and Technology Conference*, pp. 1246–1255, May 2002.
- [94] P. L. Liu and J. K. Shang, "Interfacial embrittlement by bismuth segregation in copper/tin-bismuth Pb-free solder interconnect," *Journal of Materials Research*, vol. 16, no. 6, pp. 1651–1659, 2001.
- [95] F. Hua, Z. Mei, and J. Glazer, "Eutectic Sn-Bi as an alternative to Pb-free solders," in *Proceedings of the 48th Electronic Components & Technology Conference*, pp. 277–283, May 1998.



Hindawi

Submit your manuscripts at
<http://www.hindawi.com>

